Optimization of surface-plasmon-enhanced magneto-optical effects

Nicolas Bonod

Institut Fresnel, Unité Mixte de Recherche associée au Centre National de Recherche Scientifique 6133, Faculté des sciences et techniques de Saint-Jérôme, case 161, Avenue Escadrille Normandie Niemen, 13397 Marseille cedex 20, France

Raymond Reinisch

Institut de Microélectronique, Electromagnétisme et Photonique, Unité Mixte de Recherche associée au Centre National de Recherche Scientifique 5130, Enserg, 23 rue des Martyrs, BP 257, 38016 Grenoble cedex 1, France

Evgueny Popov and Michel Nevière

Institut Fresnel, Unité Mixte de Recherche associée au Centre National de Recherche Scientifique 6133, Faculté des sciences et techniques de Saint-Jérôme, case 161, Avenue Escadrille Normandie Niemen, 13397 Marseille cedex 20, France

Received June 20, 2003; revised manuscript received November 17, 2003; accepted December 4, 2003

Kretschmann prism couplers, including magneto-optical media such as Co, Fe, and Ni, allow enhancement of the magneto-optical response, such as conversion of light polarization, thanks to the resonant excitation of surface plasmons. Since these media have high losses, they support overdamped surface plasmons. A way to get high-quality surface-plasmon resonance is to use noble-metal/ferromagnetic-metal multilayer thin films. The question that arises is, which surface-plasmon resonance leads to the largest enhancement: is it the overdamped or the high-quality one? We show that the best optimization not only depends on the orientation of the magnetic field but also on the magneto-optical coefficients. The most effective enhancer of the magneto-optical effects is the high-quality surface plasmons for the transverse orientation and may be the overdamped surface plasmons for the polar and longitudinal ones. This applies when the noble metal is gold and the magneto-optical medium is cobalt.

OCIS codes: 210.3810, 240.6680.

1. INTRODUCTION

Interaction of light with magneto-optical media leads to a rotation of the polarization vector of both the reflected and the transmitted fields, called Kerr and Faraday effects, respectively. Thus these effects involve reflection and transmission matrices.[1–8] Since magneto-optical phenomena have small magnitudes, it is of interest to enhance the magneto-optical response. Surface plasmons excited in the Kretschmann configuration[9–10] are good candidates to achieve this goal.[11] Considering magneto-optical Kretschmann prism couplers, the question of the optimization of their reflected or transmitted signal has not been dealt with yet. Two configurations are possible:

(1) The magneto-optical layer is directly on the base of the prism.[12] In this case, a difficulty arises from the fact that magneto-optical metallic media (such as Co, Fe, and Ni) have high losses, leading to an overdamped surface-plasmon resonance.

(2) As explained in Refs. 13 and 14, using noble-metal/ferromagnetic-metal multilayer thin films, instead of the ferromagnetic layer alone, leads to a high-quality factor of the surface-plasmon resonance.

It is important to realize that, due to the magneto-optical effect, one no longer deals with a TM (TM, transverse magnetic; TE, transverse electric) surface plasmon, but with a hybrid TE–TM magneto-optical surface plasmon.[15] The TM and TE electromagnetic field components (TM: H_z, E_x, E_y; TE: E_z, H_x, H_y; **E**, **H**: electric and magnetic fields) behave differently when varying the metal thickness: for the TM ones, there exists an optimum value of the metal thickness for which the surface-plasmon intensity is the largest,[11] whereas for the TE component, only the skin effect[16] is present. Consequently, using noble-metal/ferromagnetic-metal multilayer thin films has the advantage of a high-quality surface-plasmon resonance, but it has the drawback that the noble-metal layer located between the magneto-optical medium and the base of the prism attenuates the hybrid surface-plasmon amplitude due to the skin effect experienced by its TE component. In configuration 1, this skin effect does not exist, but the drawback is that the surface-plasmon resonance is overdamped. Hence the question: In view of optimizing the magneto-optical response, do we have to choose scheme 1 or scheme 2?

In order to answer this question, we first define the magneto-optical effects. We consider in Section 3 the expressions of the magneto-optical coefficients derived in Ref. 14, Eqs. 13–15. Section 4 is devoted to the rigorous solution of Maxwell equations in multilayer systems, including magneto-optical media. In Section 5, we present

rigorous numerical results concerning the optimization of magneto-optical Kretschmann prism couplers. The generality of the results obtained in this paper is discussed in Section 6.

2. DEFINITION OF THE MAGNETO-OPTICAL EFFECTS

When we apply a magnetic field to a magneto-optical medium, its dielectric permittivity tensor $[\epsilon]$ is changed; off-diagonal terms ($^{+}_{-}\epsilon_{nd}$) appear, which depend on the magnetic field orientation with respect to the principal axis of the medium. The three fundamental configurations are the polar orientation for which

$$[\epsilon]_{pol} = \begin{bmatrix} \epsilon_d & 0 & \epsilon_{nd} \\ 0 & \epsilon_d & 0 \\ -\epsilon_{nd} & 0 & \epsilon_d \end{bmatrix}, \tag{1}$$

the longitudinal orientation for which

$$[\epsilon]_{longit} = \begin{bmatrix} \epsilon_d & 0 & 0 \\ 0 & \epsilon_d & \epsilon_{nd} \\ 0 & -\epsilon_{nd} & \epsilon_d \end{bmatrix}, \tag{2}$$

and the transverse orientation for which

$$[\epsilon]_{trans} = \begin{bmatrix} \epsilon_d & \epsilon_{nd} & 0 \\ -\epsilon_{nd} & \epsilon_d & 0 \\ 0 & 0 & \epsilon_d \end{bmatrix}. \tag{3}$$

For anisotropic materials, the reflecting and transmitting behavior is described by a reflection $[r]$ and a transmission $[t]$ matrix:

$$[r] = \begin{bmatrix} r^{ss} & r^{sp} \\ r^{ps} & r^{pp} \end{bmatrix}, \tag{4a}$$

$$[t] = \begin{bmatrix} t^{ss} & t^{sp} \\ t^{ps} & t^{pp} \end{bmatrix}, \tag{4b}$$

where the right-hand part of the superscript denotes the incident polarization, and the left-hand part of the superscript denotes the polarization of the reflected or transmitted wave. We define the magneto-optical effect[14] for each element r^{ij} (respectively, t^{ij}) of the $[r]$ (respectively, $[t]$) matrix as the difference between r^{ij} calculated with $\epsilon_{nd} \neq 0$ and r^{ij} calculated with $\epsilon_{nd} = 0$:

$$\Delta r^{ij} = r^{ij}_{\epsilon_{nd}\neq 0} - r^{ij}_{\epsilon_{nd}=0} \tag{5a}$$

$$\Delta t^{ij} = t^{ij}_{\epsilon_{nd}\neq 0} - t^{ij}_{\epsilon_{nd}=0}. \tag{5b}$$

Furthermore, in Ref. 8 it has been shown that

$$|\Delta r^{sp}| = |\Delta r^{ps}|. \tag{6}$$

3. ENHANCEMENT OF THE MAGNETO-OPTICAL RESPONSE: DO WE HAVE TO CHOOSE HIGH-QUALITY OR OVERDAMPED SURFACE-PLASMON RESONANCE?

The magneto-optical prism coupler (Fig. 1), which is illuminated by a plane wave (polarization TM or TE, incidence θ_i, wavelength in vacuum λ, amplitude A_i, θ_r value of θ_i for which surface-plasmon resonance takes place), includes three layers[14]: Au, Co (the magneto-optical medium), and Au, with thicknesses e_1, e_2, e_3, respectively. The numerical values of ϵ_1, ϵ_2, ϵ_3, ϵ_M, ϵ_{nd}, e_2, and λ are those of Ref. 14. Since in such a sandwich structure, the easy magnetization direction depends on the thickness of the magneto-optical material,[14] throughout this paper, we consider the Co thickness as a given parameter having the values used in Ref. 14.

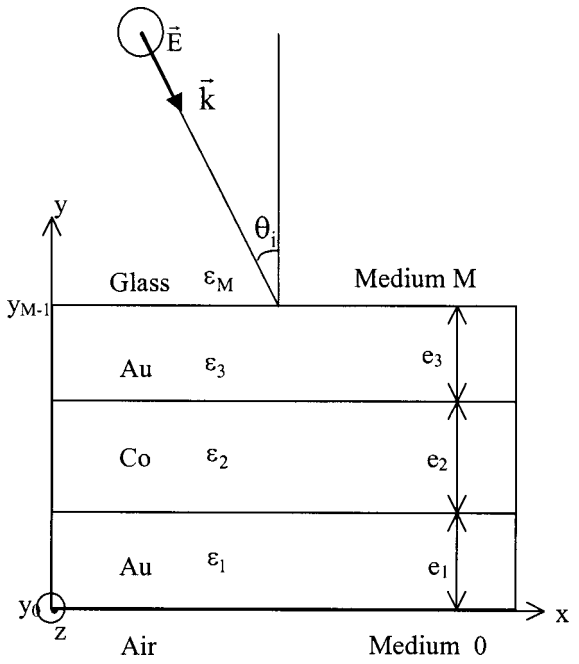

Fig. 1. Magneto-optical Kretschmann prism coupler. $\lambda_i = 647$ nm, $\epsilon_1 = \epsilon_3 = -11. + i2$, $\epsilon_2 = -11.5 + i18.3$, $\epsilon_M = 2.28$, $\epsilon_{nd} = i0.65$. The relative permittivity of the substrate is equal to 1. These numerical values are those of Ref. 14.

If the magneto-optical medium layer is thin, as shown in Ref. 14, the magneto-optical coefficients Δr^{sp} in polar and longitudinal configurations, or Δr^{pp} in transverse configuration, can be expressed as a function of the three components of the electric field calculated considering the equivalent pure gold layer of total thickness $t = e_1 + e_2 + e_3$, at the ordinate corresponding to the center of the layer of thickness, e_2, i.e., $y = e_1 + e_2/2$. The skin effect induced by the TE component E_z of the hybrid surface plasmon enters the expression of the magneto-optical coefficients derived in Ref. 14 through the product of the electric fields components appearing at their numerator in the two following magnetic orientations, that is to say, E_zE_x for the polar orientation and E_zE_y for the longitudinal orientation. In these products the x and y components of the electric field correspond to the TM polarization for which an optimization is possible.[11]

In transverse configuration, the coefficient Δr^{pp} is proportional to TM electric field components only, i.e., E_xE_y, so that it can be expected that the optimization of Δr^{pp} corresponds to the high-quality surface-plasmon resonance. But in polar and longitudinal orientations, the conclusion will depend on the relative magnitude of the skin effect and surface-plasmon resonance.

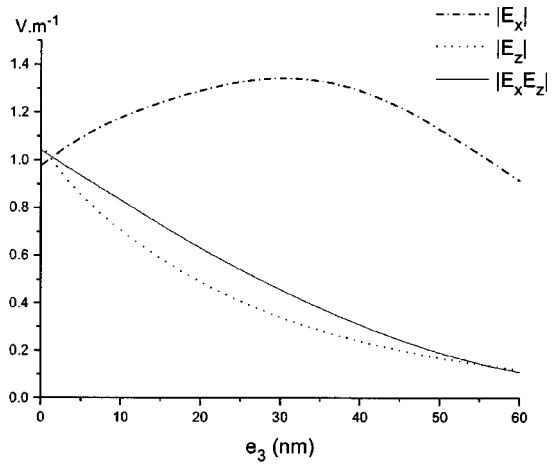

(a)

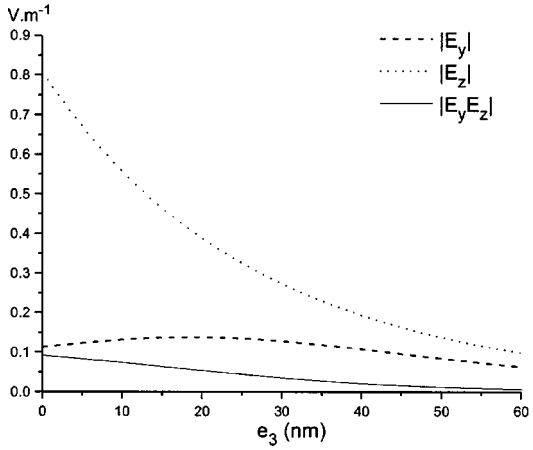

(b)

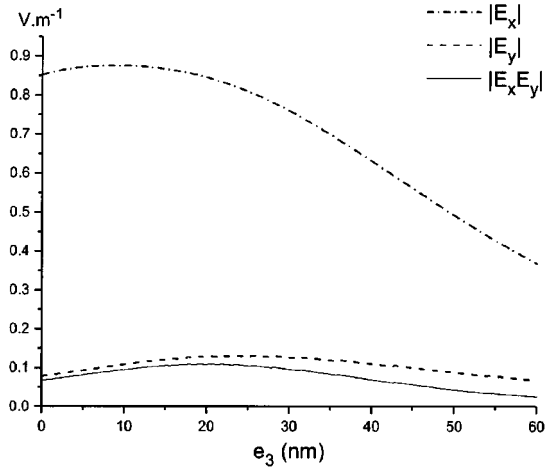

(c)

Fig. 2. Variation as a function of e_3 of (a) $|E_x|$, $|E_z|$, $|E_xE_z|$ (i.e., polar orientation) for $e_1 = 4.0$ nm, $e_2 = 1.0$ nm, (b) $|E_y|$, $|E_z|$, $|E_yE_z|$ (i.e., longitudinal orientation), and (c) $|E_x|$, $|E_y|$, $|E_xE_y|$ (i.e., transverse orientation) for $e_1 = 5.8$ nm, $e_2 = 5.7$ nm.

Using the numerical values of Ref. 14, Fig. 2 shows plots, versus e_3, of the three electric field components modulus, and of the various products of two of them. The angle of incidence is chosen such that surface-plasmon resonance occurs, i.e., $\theta_i = \theta_r$. This angle depends on the gap gold layer thickness and has to be calculated for each value of e_3. It is determined by calculating the largest value of the TM component of the electric field (E_x or E_y) when the device is illuminated in TM polarization. In polar and longitudinal magnetic configuration, at the corresponding angle of resonance θ_r, we calculate the E_z component in TE polarization.

The TE component E_z exhibits no maximum: It exponentially decreases when increasing e_3, as expected for the skin effect. The x and y electric field components have a maximum that corresponds to optimization. As seen in these figures, for the polar and longitudinal orientations, no maximum occurs for $|E_zE_x|$ and $|E_zE_y|$. It means that, although the TM components of the electric field may be optimized, the skin effect experienced by E_z prevails. Figure 2 allows us to answer the question asked in this section: In the polar and longitudinal orientations, with the values of Ref. 14, overdamped surface plasmons are the best candidates for the optimization of the magneto-optical response. Concerning the transverse orientation, the largest magneto-optical response is obtained using noble-metal/ferromagnetic-metal multilayer thin films.

The results derived in this section have been obtained considering only the product of the electric field components entering the magneto-optical coefficient Δr^{sp} and Δr^{pp} of Ref. 14. It is of interest to consider the rigorous solution of Maxwell equations in multilayer systems including magneto-optical media and to apply this formalism to the study of the magneto-optical prism coupler. Proceeding along these lines, we get the e_3 and e_1 dependences of all the elements of the reflection and transmission matrices when magneto-optical surface-plasmon resonance occurs. This allows us to perform a thorough study of the optimization of such couplers. This is the object of the next sections.

4. *S*-MATRIX PROPAGATION ALGORITHM IN ANISOTROPIC MEDIA

In this section, no simplification is made concerning the thickness of the magneto-optical layer. Thus the results obtained here are valid whatever this thickness may be.

In order to resolve Maxwell equations in such media, our work uses and extends to anisotropic media the *S*-matrix propagation algorithm[17,18] recently introduced in the electromagnetic theories of diffraction. With this tool, our computer code is free from numerical instabilities even when the thickness of the stack is much larger than the wavelength. We first show how to apply the *S*-matrix propagation algorithm to anisotropic media and how to deduce the physical observables for experimentalists.

The boundary-value problem is reduced to the numerical integration of a first-order differential equation $d\mathbf{F}(y)/dy = M(y)\mathbf{F}(y)$ similar to the one found in the differential theory of gratings.[18] We consider an incident plane wave with complex electric field vector $\mathbf{E} = \mathbf{E}_i \exp[i(\mathbf{k}_i \cdot \mathbf{r})]$ falling on a stack of layers with the wave vector in the Oxy plane. The bottom ordinate is y_0, while the top ordinate is y_{M-1} [Fig. 1]. The superstrate ($y \geqslant y_{M-1}$) is denoted M, and the substrate (y

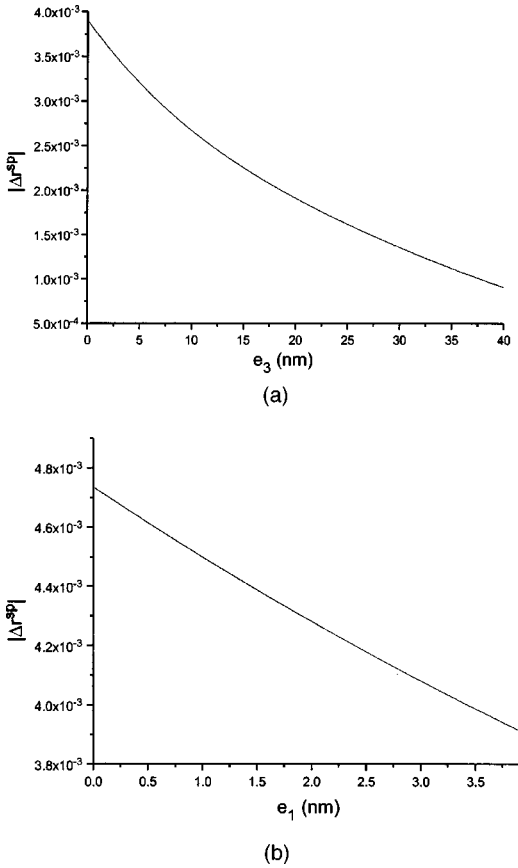

Fig. 3. Variation of $|\Delta r^{sp}|$ in the polar orientation: (a) as a function of e_3 for $e_1 = 4.0$ nm, $e_2 = 1.0$ nm (step 1), and (b) as a function of e_1 for $e_3 = e_{3,\mathrm{opt}} = 0$ nm, $e_2 = 1.0$ nm (step 2).

$\leqslant$ y0) is denoted 0. The dielectric tensors of the various layers are expressed in the $Oxyz$ basis. We denote by λ the wavelength in vacuum and by α, β the projections of the incident wave vector, respectively, onto the Ox and Oy axis. At ordinate y_i, we introduce an infinitely thin layer[18] of a medium identical to the superstrate, inside which we write the solutions $E^i = E(y_i)$ and $H^i = H(y_i)$ of the Helmholtz equation, as

$$\mathbf{E}^i = \exp(i\alpha x)[\mathbf{a}^{+(i)}\exp(i\beta_M y_i) + \mathbf{a}^{-(i)}\exp(-i\beta_M y_i)], \tag{7}$$

where $\mathbf{a}^{+(i)}$ and $\mathbf{a}^{-(i)}$ are the electric field amplitudes of the upgoing and downgoing plane waves, and β_M is the value of β in the superstrate,

$$\mathbf{H}^i = \exp(i\alpha x)[\mathbf{b}^{+(i)}\exp(i\beta_M y_i) + \mathbf{b}^{-(i)}\exp(-i\beta_M y_i)], \tag{8}$$

where $\mathbf{b}^{+(i)}$ and $\mathbf{b}^{-(i)}$ are similar vector amplitudes for the magnetic field.

In view of applying the S-matrix propagation algorithm, we first define the S matrix of a stack of anisotropic layers by

$$\begin{pmatrix} a_z^{+(M)}\exp(i\beta_M y_M) \\ b_z^{+(M)}\exp(i\beta_M y_M) \\ a_z^{-(0)} \\ b_z^{-(0)} \end{pmatrix} = S^{(M)} \begin{pmatrix} a_z^{+(0)} \\ b_z^{+(0)} \\ a_z^{-(M)}\exp(-i\beta_M y_M) \\ b_z^{-(M)}\exp(-i\beta_M y_M) \end{pmatrix} = \begin{pmatrix} S_{11} & S_{12} \\ S_{21} & S_{22} \end{pmatrix}^{(M)} \times \begin{pmatrix} a_z^{+(0)} \\ b_z^{+(0)} \\ a_z^{-(M)}\exp(-i\beta_M y_M) \\ b_z^{-(M)}\exp(-i\beta_M y_M) \end{pmatrix}, \tag{9}$$

where a_z^+, b_z^+, a_z^-, b_z^- are, respectively, the projections of $\mathbf{a}^+$, $\mathbf{b}^+$, $\mathbf{a}^-$, $\mathbf{b}^-$ onto the Oz axis, and S_{11}, S_{22}, S_{12}, S_{21} are (2×2) block matrices. Algebraic calculations lead to

$$r^{ss} = S_{12}^{(M)}(1,1), \qquad t^{ss} = S_{22}^{(M)}(1,1),$$

$$r^{pp} = S_{12}^{(M)}(2,2), \qquad t^{pp} = S_{22}^{(M)}(2,2),$$

$$r^{ps} = \frac{1}{cn_M\epsilon_0}S_{12}^{(M)}(2,1), \qquad t^{ps} = \frac{1}{cn_0\epsilon_0}S_{22}^{(M)}(2,1),$$

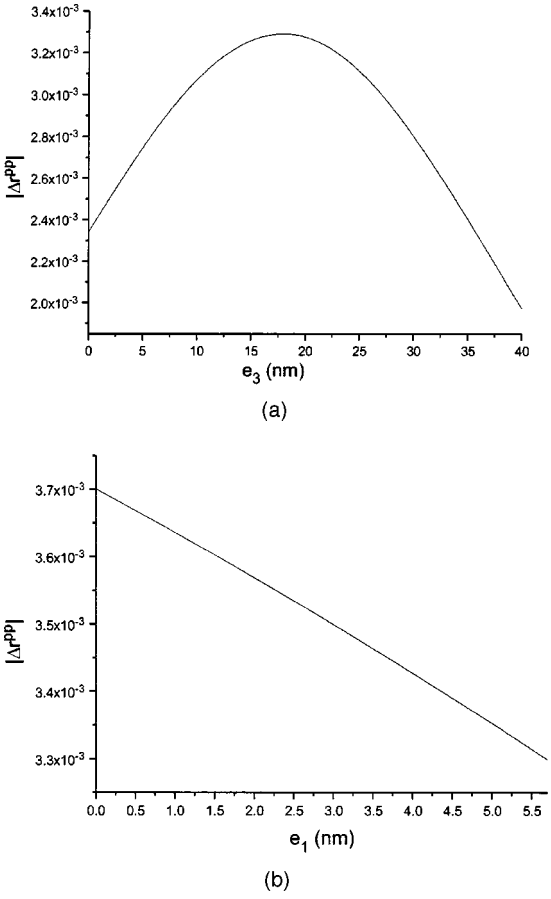

Fig. 4. Variation of $|\Delta r^{pp}|$ in the transverse orientation: (a) as a function of e_3 for $e_1 = 5.8$ nm, $e_2 = 5.7$ nm (step 1), and (b) as a function of e_1 for $e_3 = e_{3,\mathrm{opt}} = 17.9$ nm, $e_2 = 5.7$ nm (step 2).

Table 1. Values of the Set ($e_{3,opt}$, e_2, $e_{1,opt}$), θ_r, and $|\Delta r^{ij}|$, $(i,j=s,p)$[a]

Magnetic Orientation	$\lvert\Delta r^{ss}\rvert$	$\lvert\Delta r^{pp}\rvert$	$\lvert\Delta r^{sp}\rvert = \lvert\Delta r^{ps}\rvert$
Polar	$e_{1,opt} = 0.0$ nm $e_2 = 1.0$ nm $e_{3,opt} = 0.0$ nm $\lvert\Delta r^{ss}\rvert = 1.46 \times 10^{-5}$ $\theta_r = 47.8$ deg	$e_{1,opt} = 0.0$ nm $e_2 = 1.0$ nm $e_{3,opt} = 0.0$ nm $\lvert\Delta r^{pp}\rvert = 1.65 \times 10^{-5}$ $\theta_r = 54.9$ deg	$e_{1,opt} = 0.0$ nm $e_2 = 1.0$ nm $e_{3,opt} = 0.0$ nm $\lvert\Delta r^{sp}\rvert = \lvert\Delta r^{ps}\rvert = 4.7345 \times 10^{-3}$ $\theta_r = 50.9$ deg
Longitudinal	$e_{1,opt} = 0.0$ nm $e_2 = 5.7$ nm $e_{3,opt} = 0.0$ nm $\lvert\Delta r^{ss}\rvert = 4.719 \times 10^{-4}$ $\theta_r = 41.5$ deg	$e_{1,opt} = 0.0$ nm $e_2 = 5.7$ nm $e_{3,opt} = 0.0$ nm $\lvert\Delta r^{pp}\rvert = 4.9 \times 10^{-6}$ θr=41.6 deg	$e_{1,opt} = 0.0$ nm $e_2 = 5.7$ nm $e_{3,opt} = 0.0$ nm $\lvert\Delta r^{sp}\rvert = \lvert\Delta r^{ps}\rvert = 2.2073 \times 10^{-3}$ $\theta_r = 41.6$ deg
Transverse	Too small values of $\lvert\Delta r^{ss}\rvert$	$e_{1,opt} = 0.0$ nm $e_2 = 5.7$ nm $e_{3,opt} = 17.9$ nm $\lvert\Delta r^{pp}\rvert = 3.6962 \times 10^{-3}$ $\theta_r = 43.7$ deg	$\lvert\Delta r^{sp}\rvert = \lvert\Delta r^{ps}\rvert = 0$

[a] Corresponding to the optimization of the surface-enhanced magneto-optical effect, the noble metal being gold.

Table 2. Values of the Set ($e_{3,opt}$, e_2, $e_{1,opt}$), θ_r, and $|\Delta t^{ij}|$ $(i,j=s,p)$[a]

Magnetic Orientation	$\lvert\Delta t^{ss}\rvert$	$\lvert\Delta t^{pp}\rvert$	$\lvert\Delta t^{sp}\rvert$	$\lvert\Delta t^{ps}\rvert$
Polar	$e_{1,opt} = 0.0$ nm $e_2 = 1.0$ nm $e_{3,opt} = 0.0$ nm $\lvert\Delta t^{ss}\rvert = 1.45 \times 10^{-5}$ $\theta_r = 47.8$ deg	$e_{1,opt} = 0.0$ nm $e_2 = 1.0$ nm $e_{3,opt} = 47.5$ nm $\lvert\Delta t^{pp}\rvert = 4.36 \times 10^{-5}$ $\theta_r = 43.9$ deg	$e_{1,opt} = 0.0$ nm $e_2 = 1.0$ nm $e_{3,opt} = 0.0$ nm $\lvert\Delta t^{sp}\rvert = 3.1263 \times 10^{-3}$ $\theta_r = 50.8$ deg	$e_{1,opt} = 0.0$ nm $e_2 = 1.0$ nm $e_{3,opt} = 0.0$ nm $\lvert\Delta t^{ps}\rvert = 1.08480 \times 10^{-2}$ $\theta_r = 41.5$ deg
Longitudinal	$e_{1,opt} = 0.0$ nm $e_2 = 5.7$ nm $e_{3,opt} = 0.0$ nm $\lvert\Delta t^{ss}\rvert = 4.718 \times 10^{-4}$ $\theta_r = 41.5$ deg	$e_{1,opt} = 0.0$ nm $e_2 = 5.7$ nm $e_{3,opt} = 29.0$ nm $\lvert\Delta t^{pp}\rvert = 9.4 \times 10^{-6}$ $\theta_r = 43.1$ deg	$e_{1,opt} = 0.0$ nm $e_2 = 5.7$ nm $e_{3,opt} = 0.0$ nm $\lvert\Delta t^{sp}\rvert = 1.4594 \times 10^{-3}$ $\theta_r = 41.6$ deg	$e_{1,opt} = 0.0$ nm $e_2 = 5.7$ nm $e_{3,opt} = 0.0$ nm $\lvert\Delta t^{ps}\rvert = 4.3029 \times 10^{-3}$ $\theta_r = 41.7$ deg
Transverse	Too small values of $\lvert\Delta t^{ss}\rvert$	$e_{1,opt} = 1.5$ nm $e_2 = 5.7$ nm $e_{3,opt} = 34.2$ nm $\lvert\Delta t^{pp}\rvert = 1.11946 \times 10^{-2}$ $\theta_r = 43.4$ deg	$\lvert\Delta t^{sp}\rvert = 0$	$\lvert\Delta t^{ps}\rvert = 0$

[a] Corresponding to the optimization of the surface-enhanced magneto-optical effect, the noble metal being gold.

$$r^{sp} = \frac{n_M}{c\mu_0} S_{12}^{(M)}(1,2), \qquad t^{sp} = \frac{n_0}{c\mu_0} S_{22}^{(M)}(1,2), \tag{10}$$

where ϵ_0 is the permittivity of vacuum, c is the speed of light in vacuum, n_M is the refractive index of the superstrate, and n_0 is the refractive index of the substrate.

5. ENHANCEMENT OF THE MAGNETO-OPTICAL RESPONSE

In this section, we apply the S-matrix propagation algorithm to the study of the prism coupler using the numerical values of Ref. 14. As explained at the beginning of Section 3, the Co thickness is considered as a fixed parameter having the values used in Ref. 14 for the polar, longitudinal, and transverse orientations. Our interest is in the values $e_{1,opt}$ of e_1 and $e_{3,opt}$ of e_3 that yield the largest magneto-optical effect in reflection and in transmission, i.e., which yield the maximum of $|\Delta r^{ij}|$ and $|\Delta t^{ij}|$. The angle of incidence is chosen, for each value of the considered variable e_3 or e_1, such that the magneto-optical surface-plasmon resonance occurs.

For the polar, longitudinal, and transverse orientations, our study is performed in two steps:

Step 1 is the determination of $e_{3,opt}$. For this first step, we calculate the values $|\Delta r^{ij}|$ and $|\Delta t^{ij}|$ as a function of e_3. The values of e_1 and e_2 are those of Ref. 14, i.e., $e_1 = 4.0$ nm, $e_2 = 1.0$ nm for the polar orientation and $e_1 = 5.8$ nm, $e_2 = 5.7$ nm for the longitudinal and transverse orientations.

Step 2 is the determination of $e_{1,opt}$ with the $e_{3,opt}$ value determined at step 1 and with e_2 equal to 1.0 nm or 5.7

nm (depending on the magneto-optical orientation; see step 1).

Figure 3(a) is a plot, in the polar orientation, of $|\Delta r^{sp}|$ as a function of e_3 for $e_1 = 4$ nm; Fig. 3(b) represents $|\Delta r^{sp}|$ as a function of e_1 for $e_3 = e_{3,\mathrm{opt}} = 0$ nm. Similar curves are obtained for the longitudinal orientation. Figure 4 shows plots, in the transverse orientation, of $|\Delta r^{pp}|$ as a function of e_3 for $e_1 = 5.8$ nm [Fig. 4(a)] and as a function of e_1 for $e_3 = e_{3,\mathrm{opt}} = 17.9$ nm [Fig. 4(b)].

The results concerning $e_{3,\mathrm{opt}}$ and $e_{1,\mathrm{opt}}$ with the corresponding values of θ_r and $|\Delta r^{ij}|$, $|\Delta t^{ij}|$ $(i,\ j = s, p)$ are presented in Tables 1 and 2, respectively. Considering the polar and the longitudinal orientations, $e_{3,\mathrm{opt}} = e_{1,\mathrm{opt}} = 0$, except $|\Delta t^{pp}|$ for which the optimization occurs with the strongest surface-plasmon resonance. Thus for these two orientations, the maximum of $|\Delta r^{ij}|$ and $|\Delta t^{ij}|$ (except $|\Delta t^{pp}|$) only involves the overdamped surface plasmon. For the transverse orientation, the high-quality surface plasmon is brought into play since $e_{3,\mathrm{opt}} \neq 0$. Moreover, $e_{1,\mathrm{opt}}$ and $e_{3,\mathrm{opt}}$ are different whether one deals with $|\Delta r^{pp}|$ or $|\Delta t^{pp}|$. Table 1 also shows that θ_r depends on the element of the $[r]$ and $[t]$ matrices under consideration. Finally it is seen that the rigorous results obtained in this section confirm those of Section 3.

6. DISCUSSION

Magneto-optical Kretschmann prism couplers bring into play hybrid surface plasmons, which, in addition to their usual TM component, also have a TE component. As a consequence, the values of $|\Delta r^{ij}|$ and $|\Delta t^{ij}|$ result from two antagonist effects: the optimum phenomenon coming from the TM component of the magneto-optical surface plasmons and the skin effect due to its TE component. Considering the system used in Ref. 14, with Au as noble metal and Co as magneto-optical medium, we have shown that, for the polar and longitudinal orientation, the highest enhancement is obtained with overdamped surface plasmons for all the magneto-optical coefficients except $|\Delta t^{pp}|$ for which $e_{3,\mathrm{opt}} \neq 0$. This means that with gold, except for $|\Delta t^{pp}|$, it is the skin effects that dominate. Since the enhancement of the surface-plasmon TM component increases when the dielectric losses of the noble metal decrease,[11] one may wonder if the results obtained with gold are still valid with a low-loss noble metal. To answer this question, we consider the system in Fig. 1 with silver as noble metal. The results are the following: The magneto-optical coefficients for which there is a difference concerning $e_{3,\mathrm{opt}}$, as compared with Au, are $|\Delta r^{pp}|$ for the polar orientation (Fig. 5), and $|\Delta t^{ps}|$ for the polar and longitudinal orientations (Fig. 6). For these coefficients, $e_{3,\mathrm{opt}} = 0$ for Au, whereas $e_{3,\mathrm{opt}} \neq 0$ for Ag. Thus changing gold to silver modifies the respective magnitudes of the TM surface-plasmon resonance[11] and of the TE skin effect.[16] In order to get the highest enhancement, the choice of the surface-plasmon resonance, high quality or overdamped, not only depends on the different media that constitute the system at hand but, for a given prism coupler, it also depends on the magneto-optical coefficient and on the polar, longitudinal, or transverse orientation.

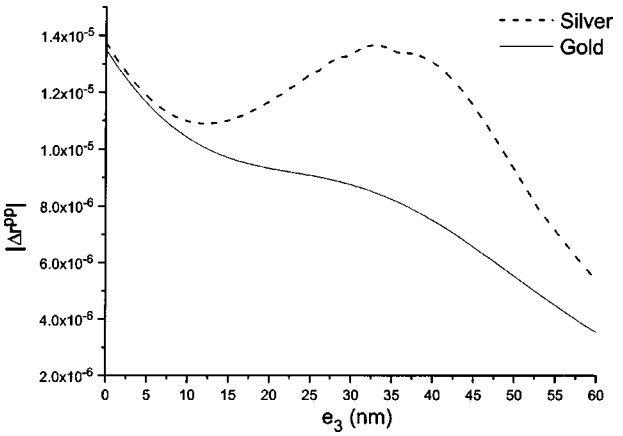

Fig. 5. Variation of $|\Delta r^{pp}|$ as a function of e_3 when the layers of thicknesses e_1 and e_3 are made of silver[19] $\epsilon_1 = \epsilon_3 = -17.6 + i0.6$, or gold $\epsilon_1 = \epsilon_3 = -11. + i2$, in the polar orientation for $e_1 = 4.0$ nm, $e_2 = 1.0$ nm. $\lambda_i = 647$ nm, $\epsilon_2 = -11.5 + i18.3$, $\epsilon_{\mathrm{M}} = 2.28$, $\epsilon_{\mathrm{nd}} = i0.65$.

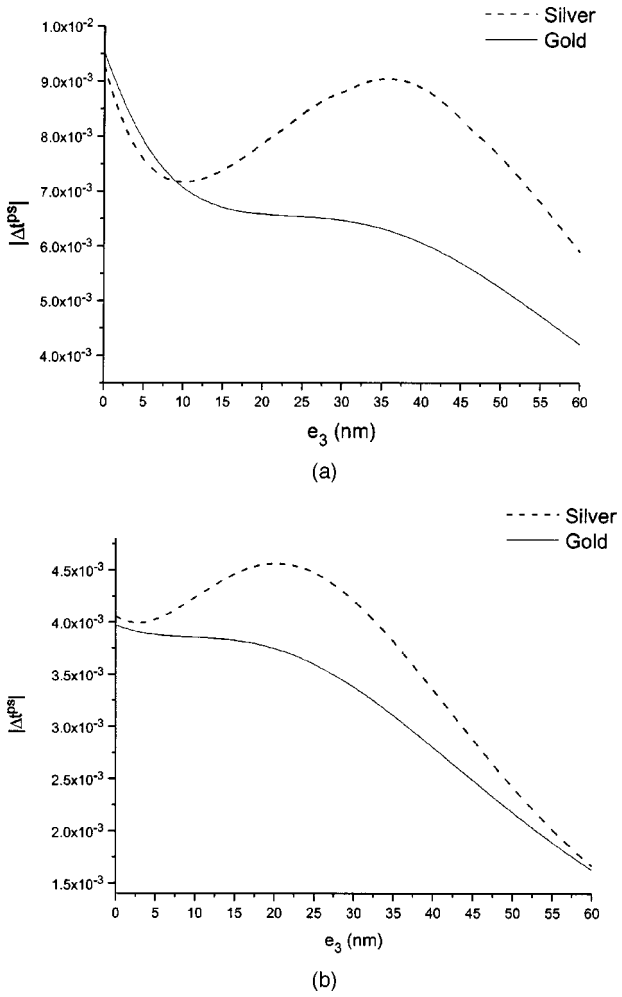

Fig. 6. Variation of $|\Delta t^{\mathrm{ps}}|$ as a function of e_3 when the layers of thicknesses e_1 and e_3 are made of silver[19] $\epsilon_1 = \epsilon_3 = -17.6 + i0.6$, or gold $\epsilon_1 = \epsilon_3 = -11. + i2$, (a) in the polar orientation ($e_1 = 4.0$ nm, $e_2 = 1.0$ nm), and (b) in the longitudinal orientation ($e_1 = 5.8$ nm, $e_2 = 5.7$ nm). $\lambda_i = 647$ nm, $\epsilon_2 = -11.5 + i18.3$, $\epsilon_{\mathrm{M}} = 2.28$, $\epsilon_{\mathrm{nd}} = i0.65$.

7. CONCLUSION

Concerning the optimization of magneto-optical prism couplers in the Kretschmann geometry, one has to be cautious. Indeed, we show in this paper that there is no general rule concerning the choice of the surface-plasmon resonance since the result depends on the relative magnitude of the surface-plasmon resonance and of the skin effect, both phenomena being induced by the hybrid TE–TM magneto-optical surface plasmon. For the transverse orientation, optimization is achieved with high-quality surface plasmons. This is due to the fact that no rotation of polarization occurs. But for the polar and longitudinal orientations, overdamped surface plasmons may be the best candidates in view of the optimization of the magneto-optical coefficients. This is, for example, the case for the prism coupler considered in Ref. 14. The study developed in this paper is valid for any magneto-optical planar multilayer structure. The results reported here point to the important role played by the TE component of the hybrid surface plasmon in the optimization process.

REFERENCES

1. R. P. Hunt, "Magneto-optic scattering from thin solid films," J. Appl. Phys. **38**, 1652–1671 (1967).
2. J. Zak, E. R. Moog, C. Liu, and S. D. Bader, "Universal approach to magneto-optics," J. Magn. Magn. Mater. **89**, 107–123 (1990).
3. S. Visnovsky, "Magneto-optical ellipsometry," Czech. J. Phys. B **36**, 625–650 (1986).
4. J. Zak, E. R. Moog, C. Liu, and S. D. Bader, "Magneto-optics of multilayers with arbitrary magnetization directions," Phys. Rev. B **43**, 6423–6429 (1991).
5. C.-Y. You and S.-C. Shin, "Derivation of simplified analytic formulae for magneto-optical Kerr effects," Appl. Phys. Lett. **69**, 1315–1317 (1996).
6. C.-Y. You and S.-C. Shin, "Generalized analytic formulae for magneto-optical Kerr effects," J. Appl. Phys. **84**, 541–546 (1998).
7. Z. Q. Qiu and S. D. Bader, "Surface magneto-optic Kerr effect (SMOKE)," J. Magn. Magn. Mater. **200**, 664–678 (1999).
8. R. Reinisch, M. Nevière, G. Tayeb, and E. Popov, "Symmetry relation for reflection and transmission coefficients of magneto-optic systems," Opt. Commun. **205**, 59–70 (2002).
9. H. Raether, *Surface Plasmons*, Vol. 11 of Springer Tracts in Modern Physics (Springer-Verlag, New York, 1988).
10. H. Raether, in *Surface Polaritons*, V. M. Agranovitch and D. L. Mills, eds. (North Holland, Amsterdam, 1982), Chap. 9.
11. M. Nevière, E. Popov, R. Reinisch, and G. Vitrant, *Electromagnetic Resonances in Nonlinear Optics* (Gordon and Breach, London, 2000).
12. P. E. Fergusson, O. M. Stafsudd, and R. F. Wallis, "Enhancement of the transverse Kerr magneto-optic effect by surface magneto-plasma waves," Physica B **89**, 91–94 (1977).
13. V. I. Safarov, V. A. Kosobukin, C. Hermann, G. Lampel, J. Peretti, and C. Marlière, "Magneto-optical effects enhanced by surface plasmons in metallic multilayer films," Phys. Rev. Lett. **73**, 3584–3587 (1994).
14. C. Hermann, V. A. Kosobukin, G. Lampel, J. Peretti, V. I. Safarov, and P. Bertrand, "Surface-enhanced magneto-optics in metallic multilayer films," Phys. Rev. B **64**, 235422 (2001).
15. K. W. Chiu and J. J. Quinn, "Magneto-plasma surface waves in solids," Nuovo Cimento B **10**, 1–20 (1972).
16. R. E. Collin, *Field Theory of Guided Waves*, 2nd ed. (IEEE, New York, 1991).
17. L. Li, "Formulation and comparison of two recursive matrix algorithms for modeling layered diffraction gratings," J. Opt. Soc. Am. A **13**, 1024–1035 (1996).
18. M. Nevière and E. Popov, *Light Propagation in Periodic Media; Differential Theory and Design* (Marcel Dekker, New York, 2003).
19. B. H. Billings, ed., *American Institute of Physics Handbook*, 2nd ed. (McGraw-Hill, New York, 1963).